

Electronic Supplementary Information

Incorporation of metal-organic framework UiO-66 into porous polymer monoliths to enhance the chromatographic separation of small molecules

Yan-Yan Fu, Cheng-Xiong Yang and Xiu-Ping Yan*

State Key Laboratory of Medicinal Chemical Biology, and Research Center for
Analytical Sciences, College of Chemistry, Nankai University, 94 Weijin Road,
Tianjin 300071, China

EXPERIMENTAL SECTION

Materials and reagents

All chemicals and reagents used were at least of analytical grade. Ultrapure water was purchased from Tianjin Wahaha Foods Co. Ltd. Zirconium chloride ($ZrCl_4$) was purchased from J&K Scientific Ltd. (Beijing, China). Terephthalic acid, naphthalene, fluorene, pyrene, chrysene, acetanilide, 4-fluoroaniline, 2-nitroaniline, 1-naphthylamine, resorcinol, *m*-cresol, 2,6-dimethylphenol, 2,6-dichlorophenol, 1-naphthol, 1-methylnaphthalene, 1-chloronaphthalene, 2,2'-Azobis(2-methylpropionitrile) (AIBN), ethylene dimethacrylate (EDMA), and methylacrylic acid (MAA) were purchased from Shanghai Aladdin Chemistry Co. Ltd. (Shanghai, China). Polyethylene glycol (PEG 6000) was purchased from Sinopharm Chemical Reagent Co. Ltd. (Shanghai, China). Acetic acid was purchased from Tianjin Chemical Reagent No. 1 Plant (Tianjin, China). Thiourea and benzene were purchased from Guangfu Fine Chemical Research Institute (Tianjin, China). Methanol (MeOH), ethanol, acetonitrile (ACN), and *N,N*-dimethylformamide (DMF) were purchased from Concord Fine Chemical Research Institute (Tianjin, China).

Instrumentation

Scanning electron microscopy (SEM) images were recorded on a Shimadzu SS-550 scanning electron microscope at 15.0 kV. A Magna-560 spectrometer (Nicolet, Madison, WI) was used to record the Fourier transform infrared (FT-IR) spectra ($4000-400\text{ cm}^{-1}$) in KBr plate. X-ray diffraction (XRD) patterns were recorded on a D/max-2500 diffractometer (Rigaku, Japan) using $Cu_{K\alpha}$ radiation ($\lambda = 1.5418\text{ \AA}$). Brunauer-Emmett-Teller (BET) surface area, pore volume and pore

size distribution were measured on a NOVA 2000e surface area and pore size analyzer (Quantachrome, Florida, FL, USA) using nitrogen adsorption at 77 K in the range $0.02 \leq P/P_0 \leq 0.20$, respectively. X-ray photoelectron spectroscopy (XPS) measurements were performed on an Axis Ultra DLD (Kratos Analytical Ltd. Britain).

A chromatographic system consisting of a Waters 510 HPLC pump and a 486 tunable absorbance detector was used to perform all HPLC separations. Data acquisition and processing were carried out on a N2000 chromatography data system. The Ameritech CO-5060 column (± 0.1 °C) heater was used to control the column temperature during HPLC separation.

Synthesis and activation of UiO-66 crystals

UiO-66 crystals were synthesized according to Schaate *et al.*¹ Typically, ZrCl₄ (0.080 g, 0.343 mmol), terephthalic acid (0.057 g, 0.343 mmol) and 0.6 mL acetic acid were mixed with 20 mL DMF in a Teflon-lined bomb. The bomb was sealed and placed in an oven at 120 °C for 24 h. After cooling down to room temperature, the white precipitates were obtained by centrifugation. After washing with DMF for three times and then ethanol, the UiO-66 crystals were obtained by centrifuging. Finally, the UiO-66 crystals were activated in vacuum at 60 °C for 12 h.

Preparation of UiO-66 incorporated poly (MAA-co-EDMA) monolith

For the fabrication of UiO-66 incorporated poly (MAA-co-EDMA) monolith, UiO-66 powder was dispersed in DMF to create a white and homogeneous dispersion at a concentration of 5, 10 or 15 mg mL⁻¹ under ultrasonication for 2 h. Then, 1270 µL of UiO-66 dispersion was added into the poly (MAA-co-EDMA) precursor containing 35 µL monomer MAA, 400 µL crosslinker EDMA and 400 mg porogen PEG 6000. After the above mixture was ultrasonicated for 0.5 h, 10 mg

initiator AIBN was added and another 5 min of ultrasonication was need to dissolve AIBN. Then the stainless-steel column tube (70.0 mm × 4.6 mm i.d.) was filled with the polymerization mixtures by a syringe and sealed at both ends. After polymerization at 60 °C for 24 h, the column was washed with methanol to remove porogen and unreacted monomer. For UiO-66 dispersion concentration studies, the concentration of UiO-66 dispersion varied from 5 to 15 mg mL⁻¹, which was the upper limit dispersion in DMF after ultrasonication for 2 h.

For comparison, the blank monolithic column was prepared in parallel by adding DMF instead of UiO-66 dispersion into polymerization mixture. The monolithic materials were also synthesized in centrifugal tube and were dried under vacuum for 12 h after Soxhlet extraction with MeOH for FT-IR, SEM and N₂ adsorption characterizations.

Calculation of thermodynamic parameters

To evaluate the thermodynamics for the transfer of the solutes from the mobile phase to the stationary phase of UiO-66 incorporated poly (MAA-co-EDMA) monolith, gibbs free energy change (ΔG , KJ mol⁻¹), enthalpy change (ΔH , KJ mol⁻¹) and entropy change (ΔS , J mol⁻¹ K⁻¹) were measured through HPLC experiments carried out at six different temperatures in the range of 25–55 °C.² The mobile phase was preheated to the same temperature as the column in a water bath during HPLC separation. ΔG , ΔH and ΔS were calculated according to the following equations (eq 1 and eq 2).

$$\ln k' = -\frac{\Delta H}{RT} + \frac{\Delta S}{R} + \ln \Phi \quad (1)$$

$$\Delta G = \Delta H - T\Delta S \quad (2)$$

where k' is retention factor, R is gas constant, T is absolute temperature and Φ is the phase ratio. k'

was calculated according to eq 3:

$$k' = (t - t_0) / t_0 \quad (3)$$

where t is the retention time and the t_0 is the column void time which was determined by injecting a small plug of thiourea and recording the perturbation signals. Φ was calculated according to eq 4:

$$\Phi = V_S / V_0 \quad (4)$$

where the volume of the stationary phase in the column: V_S was calculated based on eq 5, while the void volume of the column: V_0 (1.32 mL) was evaluated according to eq 6.

$$V_S = V_{\text{COL}} - V_0 \quad (5)$$

$$V_0 = t_0 \times F \quad (6)$$

where V_{COL} is the geometrical volume of the column, and F is the flow rate of the mobile phase.

Calculation of selectivity factors ($\alpha_{B/A}$)

The selectivity factors for analytes A and B on the UiO-66 incorporated poly (MAA-co-EDMA) monolith were calculated from chromatogram according to eq 7:

$$\alpha_{B/A} = \frac{t_B - t_0}{t_A - t_0} \quad (7)$$

where t_A and t_B are the retention times of analytes A and B, respectively. t_0 is the column void time.

Calculation of permeability

The permeability B_0 of the UiO-66 incorporated poly (MAA-co-EDMA) monolith was calculated using the hydrodynamic data from the Darcy's law³:

$$\frac{\Delta P}{L} = \frac{u\mu}{B_0} \quad (8)$$

where ΔP stands for back pressure (Pa), L for column length (m), u for superficial velocity (m s⁻¹), μ for mobile phase viscosity (Pa s), and B_0 for permeability (m²).

REFERENCES

- 1 A. Schaate, P. Roy, A. Godt, J. Lippke, F. Waltz, M. Wiebcke, P. Behrens, *Chem. Eur. J.*, 2011, **17**, 6643.
- 2 M. Śliwka-Kaszyńska, K. Jaszczółt, D. Witt, J. Rachoń, *J. Chromatogr. A*, 2004, **1055**, 21.
- 3 C. Martin, J. Coyne, G. Carta, *J. Chromatogr. A*, 2005, **1069**, 43.
- 4 P. S. Bárcia, D. Guimarães, P. A. P. Mendes, J. A. C. Silva, V. Guillerm, H. Chevreau, C. Serre, A. E. Rodrigues, *Microporous Mesoporous Mater.*, 2011, **139**, 67.

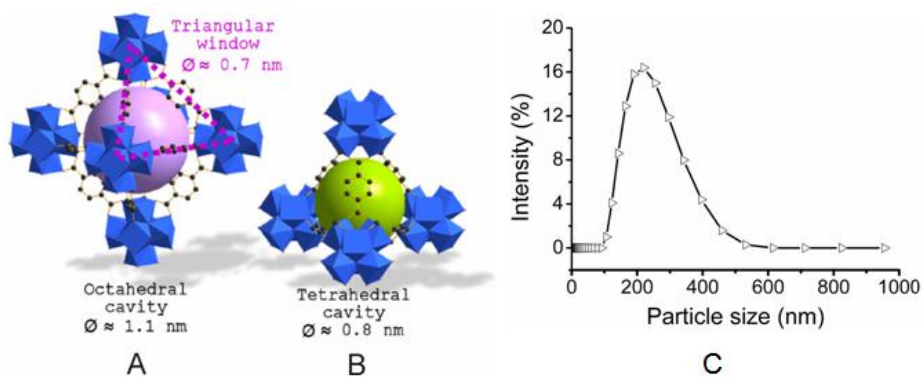


Fig. S1 View of the (A) octahedral and (B) tetrahedral cavities in the highly porous UiO-66. Zirconium polyhedral and carbon atoms are in blue and black, respectively. The free diameters of the octahedral and tetrahedral cavities are represented through purple and green spheres, respectively.⁴ (C) Particle size distribution of UiO-66.

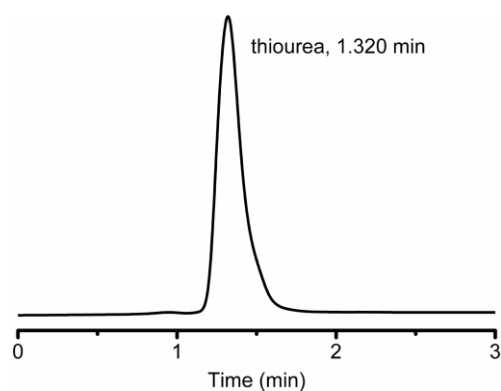


Fig. S2 Chromatogram of thiourea on UiO-66 incorporated monolith.

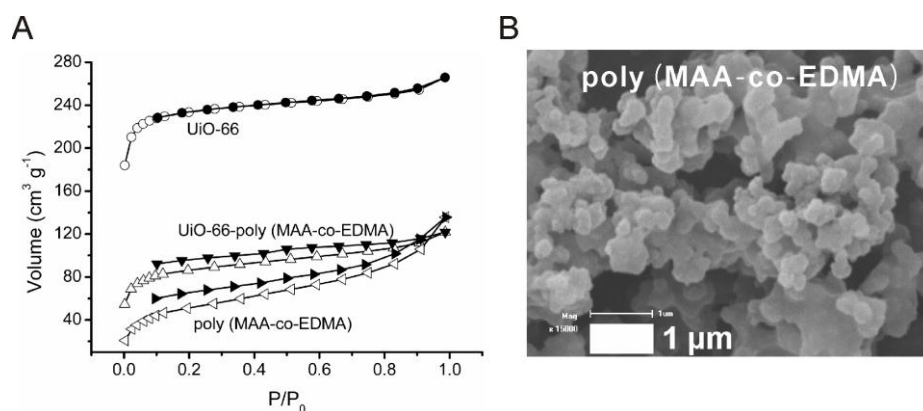


Fig. S3 (A) N_2 adsorption-desorption isotherms (hollow: adsorption, solid: desorption) of UiO-66, poly (MAA-co-EDMA) monolith and UiO-66 incorporated poly (MAA-co-EDMA) monolith; (B) SEM image of poly (MAA-co-EDMA) monolith.

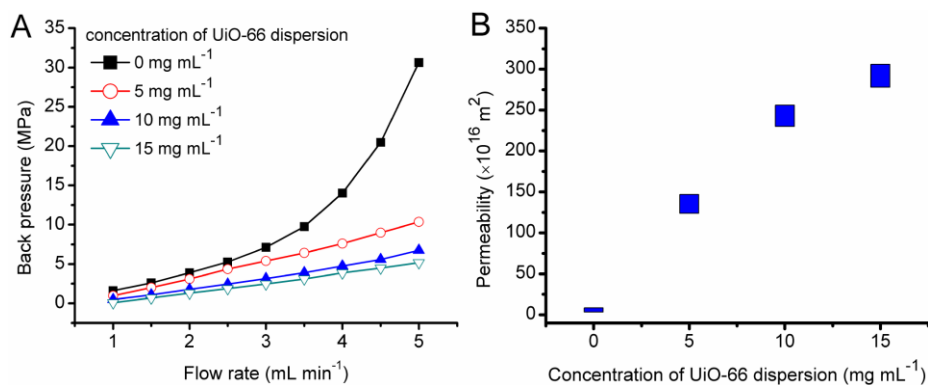


Fig. S4 (A) Effect of the flow rate on the back pressure; (B) Permeability of the monoliths with different concentrations of UiO-66 dispersion. Conditions: column, 70.0 mm × 4.6 mm i.d., mobile phase: 100% ACN. Permeability was calculated from eq 8.

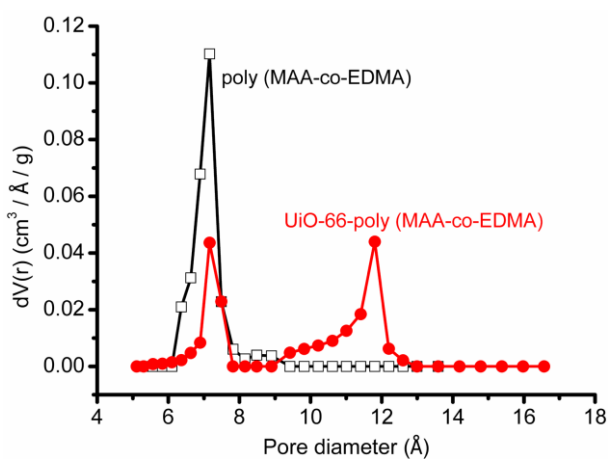


Fig. S5 Pore diameter of poly (MAA-co-EDMA) and UiO-66-poly (MAA-co-EDMA) calculated by DFT method.

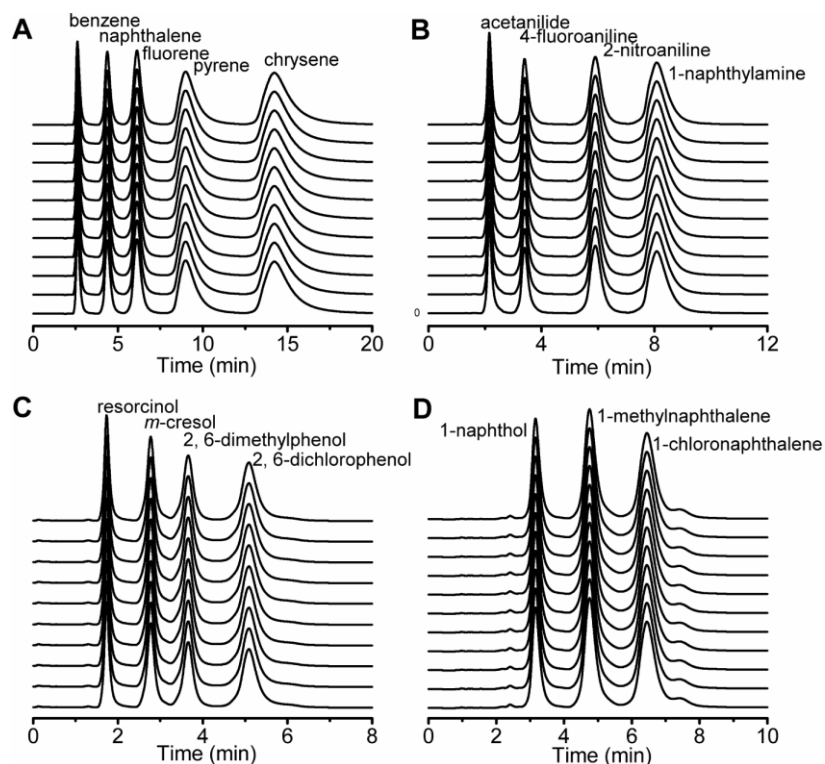


Fig. S6 HPLC chromatograms on UiO-66 (10 mg mL^{-1}) incorporated poly (MAA-co-EDMA) monolithic column ($70.0 \text{ mm} \times 4.6 \text{ mm i.d.}$) for eleven replicate separations of: (A) PAHs using ACN/ H_2O (50:50) as the mobile phase; (B) aniline series using ACN/ H_2O (35:65) as the mobile phase; (C) phenol series using ACN/ H_2O (40:60) as the mobile phase; (D) naphthyl substitutes using ACN/ H_2O (50:50) as the mobile phase. Conditions: mobile flow rate, 1.0 mL min^{-1} ; UV detection at 254 nm (A, B, D) and 280 nm (C).

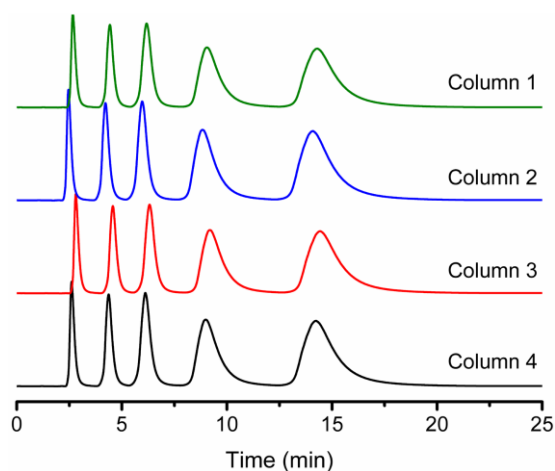


Fig. S7 HPLC chromatograms of neutral PAHs on four batches of UiO-66 incorporated

monoliths.

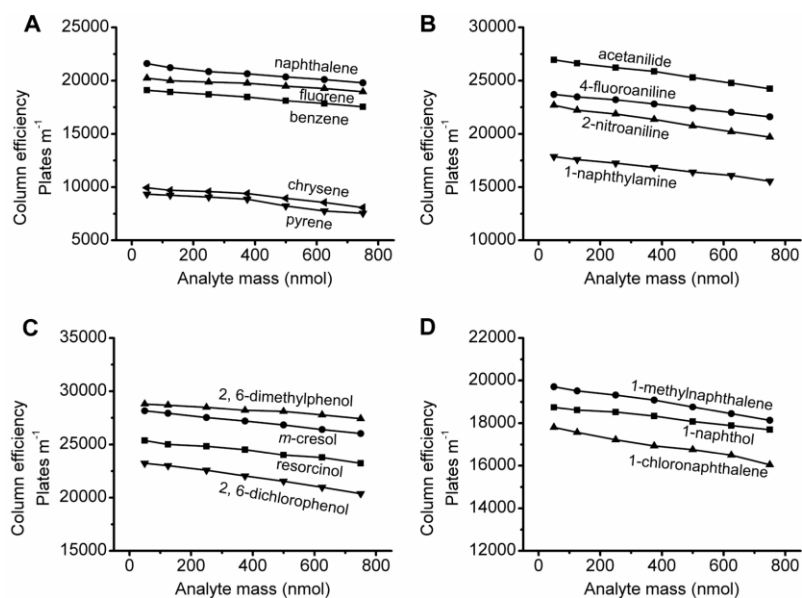


Fig. S8 Effects of injected mass on the column efficiency for: (A) PAHs; (B) aniline series; (C)

phenol series; (D) naphthyl substitutes. Conditions as shown in Fig. S6.

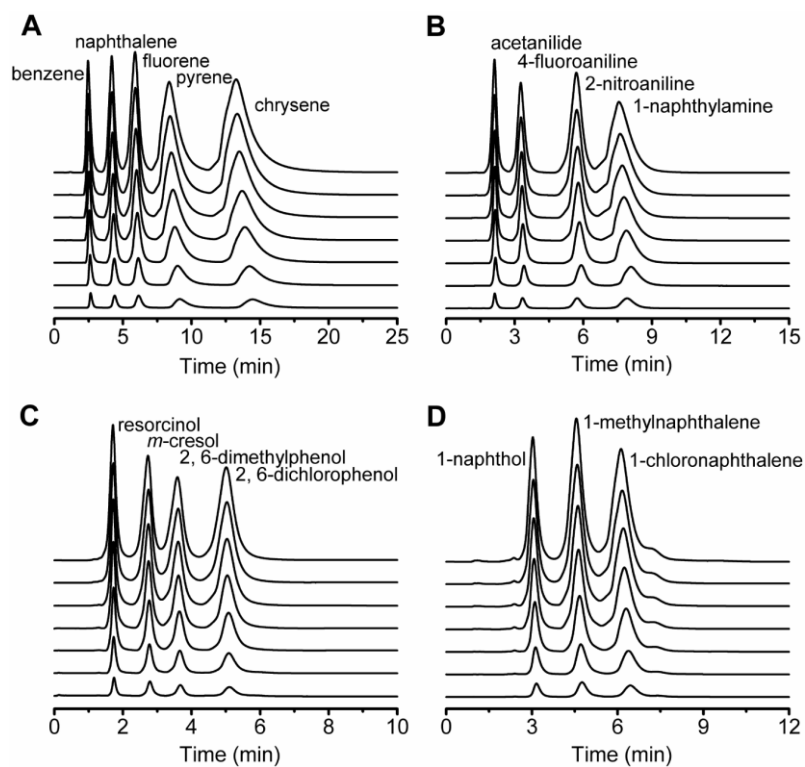


Fig. S9 Effect of injected analyte mass on the HPLC separation of (A) PAHs, (B) aniline series, (C)

phenol series and (D) naphthyl substitutes on UiO-66 (10 mg mL^{-1}) incorporated poly (MAA-co-EDMA). Conditions as shown in Fig. S6.

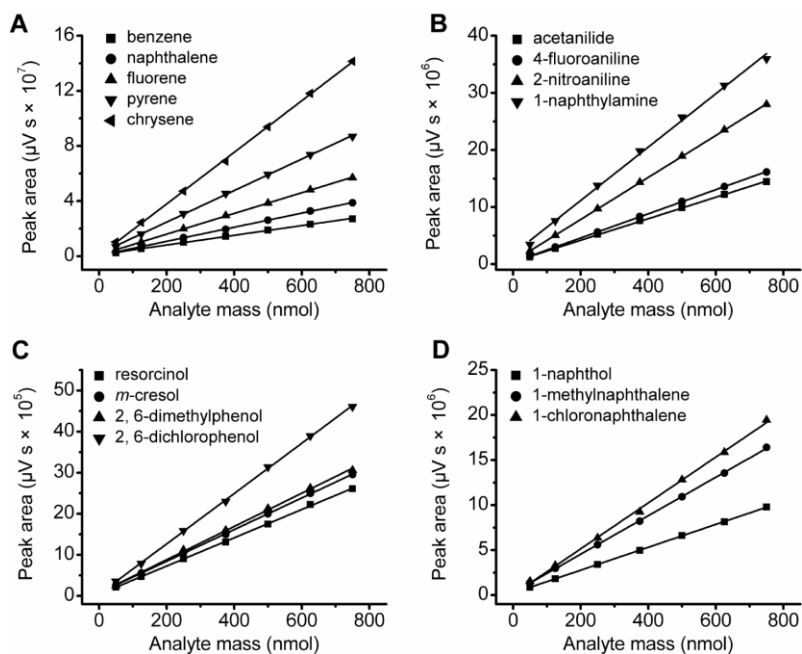


Fig. S10 Effects of injected analyte mass on the peak area: (A) PAHs; (B) aniline series; (C) phenol series; (D) naphthyl substitutes on UiO-66 (10 mg mL^{-1}) incorporated poly (MAA-co-EDMA). Conditions as shown in Fig. S6.

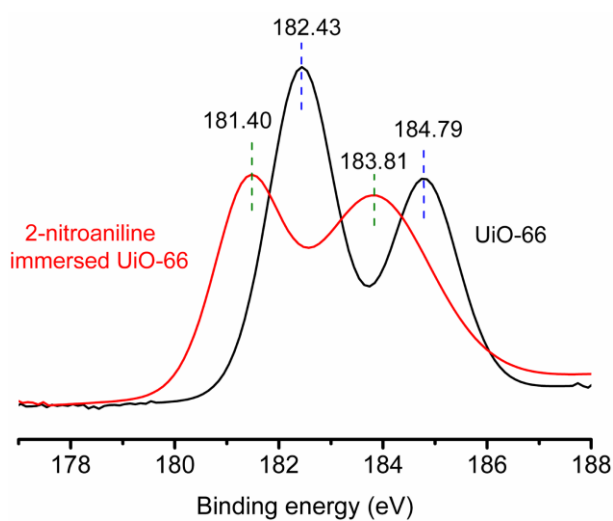


Fig. S11 XPS spectra of UiO-66 and 2-nitroaniline immersed UiO-66.

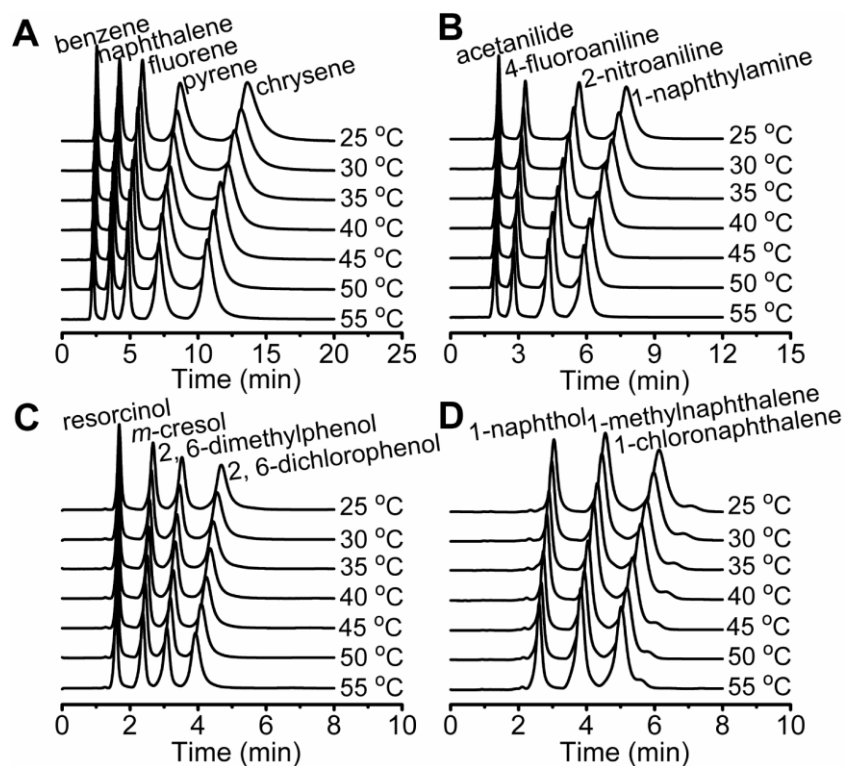


Fig. S12 Effect of temperature on UiO-66 incorporated poly (MAA-co-EDMA) monolithic column for the separation of (A) PAHs, (B) aniline series, (C) phenol series, and (D) naphthyl substitutes. Conditions: column, 70.0 mm × 4.6 mm i.d., flow rate, 1.0 mL min⁻¹; UV detector at 254 nm (A, B, and D) and 280 nm (C).

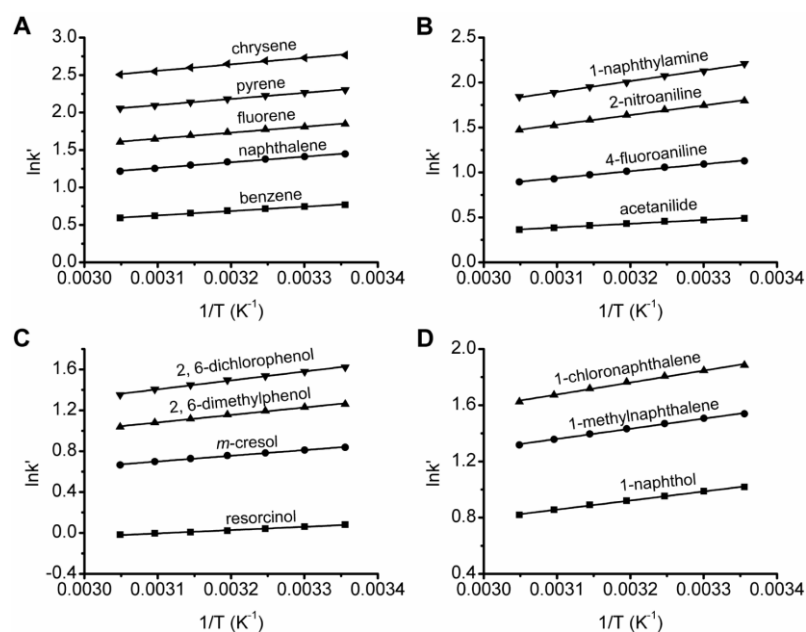


Fig. S13 Van't Hoff plots for PAHs (A), aniline series (B), phenol series (C), and naphthyl substitutes (D) on the UiO-66 incorporated poly (MAA-co-EDMA) monolithic column. Conditions as shown in Fig. S6.

Table S1 Column efficiency of all the analytes on the monolith without UiO-66 incorporation

Analyte	benzene	naphthalene	fluorene	pyrene
Column efficiency (plates m ⁻¹)	7659	5688	5282	2967
Analyte	chrysene	acetanilide	4-fluoroaniline	2-nitroaniline
Column efficiency (plates m ⁻¹)	3106	8218	7664	7129
Analyte	1-naphthylamine	resorcinol	<i>m</i> -cresol	2,6-dimethylphenol
Column efficiency (plates m ⁻¹)	4794	8096	7153	5992
Analyte	2,6-dichlorophenol	1-naphthol	1-methylnaphthalene	1-chloronaphthalene
Column efficiency (plates m ⁻¹)	4219	6427	5693	4307

Table S2 Effect of the concentration of UiO-66 dispersion (C , mg mL^{-1}) on asymmetry factor (A_s) and resolution (R_s) of PAHs: benzene (1), naphthalene (2), fluorene (3), pyrene (4), chrysene (5); aniline series: acetanilide (a), 4-fluoroaniline (b), 2-nitroaniline (c), 1-naphthylamine (d); phenol series: resorcinol (1'), *m*-cresol (2'), 2,6-dimethylphenol (3'), 2,6-dichlorophenol (4'); and naphthyl substitutes: 1-naphthol (a'), 1-methylnaphthalene (b'), 1-chloronaphthalene (c')

Analyte	$C_{\text{UiO-66}}$ (mg mL^{-1})	A_s^1	A_s^2	A_s^3	A_s^4	A_s^5	$R_s^{2/1}$	$R_s^{3/2}$	$R_s^{4/3}$	$R_s^{5/4}$
PAHs	0	1.49	0.90	1.07	1.37	1.62	1.09	0.61	0.75	0.82
	5	1.52	1.10	1.19	1.54	1.76	1.29	0.77	0.85	0.93
	10	1.56	1.23	1.24	1.82	1.89	3.10	2.14	1.86	1.96
	15	2.50	2.32	1.90	2.25	2.27	3.47	2.32	2.02	2.14

Analyte	$C_{\text{UiO-66}}$ (mg mL^{-1})	A_s^a	A_s^b	A_s^c	A_s^d	$R_s^{b/a}$	$R_s^{c/b}$	$R_s^{d/c}$
Aniline series	0	1.35	1.19	0.96	1.13	1.30	1.27	0.72
	5	1.38	1.26	1.01	1.24	1.55	1.61	0.88
	10	1.49	1.33	1.15	1.34	3.05	3.64	1.85
	15	1.52	1.72	1.59	1.80	3.30	4.07	1.97

Analyte	$C_{\text{UiO-66}}$ (mg mL^{-1})	$A_s^{1'}$	$A_s^{2'}$	$A_s^{3'}$	$A_s^{4'}$	$R_s^{2'/1'}$	$R_s^{3'/2'}$	$R_s^{4'/3'}$
Phenol series	0	1.12	0.83	0.92	1.30	1.50	0.50	0.72
	5	1.24	0.96	0.96	1.34	1.28	0.62	0.75
	10	1.27	1.19	1.00	1.37	3.31	2.03	2.28
	15	1.97	1.77	1.78	2.49	3.57	2.14	1.68

Analyte	$C_{\text{UiO-66}}$ (mg mL^{-1})	$A_s^{a'}$	$A_s^{b'}$	$A_s^{c'}$	$R_s^{b'/a'}$	$R_s^{c'/b'}$
Naphthyl substitutes	0	0.95	1.15	1.57	0.75	0.73
	5	1.36	1.21	1.60	0.99	0.81
	10	1.35	1.36	1.64	2.47	1.82
	15	1.96	1.75	2.31	2.78	1.83

Table S3 Precision for eleven replicate separations of PAHs, aniline series, phenol series and naphthyl substitutes on the UiO-66 (10 mg mL⁻¹) incorporated poly (MAA-co-EDMA) monolithic column calculated from Fig. S6

Analyte	RSD (%) (n=11)			
	t	Peak area	Peak height	W _{1/2}
benzene	0.24	1.49	1.17	0.39
naphthalene	0.10	0.56	0.99	0.25
fluorene	0.15	0.46	0.65	0.64
pyrene	0.10	0.49	0.17	0.48
chrysene	0.23	0.48	1.00	0.92
acetanilide	0.15	0.50	0.63	0.72
4-fluoroaniline	0.04	0.87	0.74	0.19
2-nitroaniline	0.02	0.80	1.85	0.24
1-naphthylamine	0.07	0.48	0.57	1.09
resorcinol	0.21	0.33	0.84	1.00
<i>m</i> -cresol	0.16	0.54	0.82	0.59
2,6-dimethylphenol	0.10	0.44	0.35	0.22
2,6-dichlorophenol	0.13	0.35	0.63	0.24
1-naphthol	0.27	1.06	1.02	0.37
1-methylnaphthalene	0.19	0.94	0.64	0.27
1-chloronaphthalene	0.17	0.82	0.36	0.29

Table S4 Selectivity of the PAHs (benzene (1), naphthalene (2), fluorine (3), pyrene (4), chrysene (5)), basic aniline series (acetanilide (a), 4-fluoroaniline (b), 2-nitroaniline (c), 1-naphthylamine (d)), acid phenol series (resorcinol (1'), *m*-cresol (2'), 2,6-dimethylphenol (3'), 2,6-dichlorophenol (4')) and naphthyl substitutes (1-naphthol (a'), 1-methylnaphthalene (b'), 1-chloronaphthalene (c')) on the UiO-66 incorporated poly (MAA-co-EDMA) monolithic column calculated from Fig. S6

Analyte mass /nmol	Selectivity (α)											
	PAH				Aniline series			Phenol series			Naphthyl substitutes	
	2/1	3/2	4/3	5/4	b/a	c/b	d/c	2'/1'	3'/2'	4'/3'	b'/a'	c'/b'
50	1.95	1.49	1.53	1.64	1.91	1.95	1.43	2.12	1.45	1.50	1.68	1.43
125	1.97	1.49	1.53	1.64	1.92	1.96	1.42	2.12	1.45	1.50	1.68	1.43
250	2.00	1.49	1.52	1.64	1.90	1.97	1.41	2.12	1.45	1.50	1.68	1.42
375	2.00	1.49	1.51	1.64	1.89	1.98	1.40	2.12	1.45	1.51	1.69	1.42
500	2.03	1.50	1.50	1.64	1.89	1.98	1.40	2.12	1.45	1.51	1.68	1.42
625	2.04	1.50	1.50	1.64	1.88	1.98	1.39	2.12	1.45	1.51	1.68	1.42
750	2.05	1.50	1.49	1.64	1.88	1.98	1.38	2.12	1.45	1.51	1.69	1.42

Table S5 Selectivity calculated from Fig. 4 of the PAHs (benzene (1), naphthalene (2), fluorine (3), pyrene (4), chrysene (5)), basic aniline series (acetanilide (a), 4-fluoroaniline (b), 2-nitroaniline (c), 1-naphthylamine (d)), acid phenol series (resorcinol (1'), *m*-cresol (2'), 2,6-dimethylphenol (3'), 2,6-dichlorophenol (4')) and naphthyl substitutes (1-naphthol (a'), 1-methylnaphthalene (b'), 1-chloronaphthalene (c')) on the UiO-66 incorporated poly (MAA-co-EDMA) monolith in the temperature range of 25-55 °C

$T/^\circ\text{C}$	Selectivity (α)											
	PAH				Aniline series			Phenol series			Naphthyl substitutes	
	2/1	3/2	4/3	5/4	b/a	c/b	d/c	2'/1'	3'/2'	4'/3'	b'/a'	c'/b'
25	1.97	1.50	1.53	1.63	1.89	1.95	1.43	2.13	1.45	1.43	1.68	1.42
30	1.95	1.49	1.55	1.62	1.87	1.92	1.43	2.11	1.45	1.42	1.68	1.42
35	1.94	1.48	1.55	1.61	1.82	1.90	1.43	2.10	1.46	1.41	1.68	1.41
40	1.92	1.48	1.56	1.60	1.79	1.87	1.44	2.07	1.45	1.40	1.68	1.41
45	1.90	1.48	1.56	1.59	1.76	1.84	1.44	2.04	1.45	1.39	1.68	1.40
50	1.88	1.47	1.56	1.58	1.74	1.81	1.45	2.03	1.45	1.38	1.68	1.40
55	1.87	1.46	1.57	1.57	1.72	1.78	1.45	2.00	1.45	1.37	1.68	1.40

Table S6 Values of ΔG , ΔH , ΔS and γ^2 (γ refers to the linear correlation coefficient of $\ln k'-1/T$ plot) for all the analytes

Analyte	$\Delta H/\text{KJ mol}^{-1}$	$\Delta S/\text{J mol}^{-1} \text{K}^{-1}$	$\Delta G/\text{KJ mol}^{-1}$	γ^2
benzene	-4.87 ± 0.19	-3.07 ± 0.61	-4.03 ± 0.19	0.9911
naphthalene	-6.26 ± 0.21	-2.12 ± 0.68	-5.68 ± 0.21	0.9931
fluorene	-6.57 ± 0.22	0.19 ± 0.71	-6.62 ± 0.22	0.9932
pyrene	-6.79 ± 0.15	3.21 ± 0.47	-7.67 ± 0.15	0.9972
chrysene	-7.14 ± 0.25	5.94 ± 0.82	-8.76 ± 0.25	0.9924
acetanilide	-3.46 ± 0.16	-0.69 ± 0.52	-3.27 ± 0.16	0.9870
4-fluoroaniline	-6.43 ± 0.19	-5.34 ± 0.61	-4.97 ± 0.19	0.9948
2-nitroaniline	-8.93 ± 0.22	-8.15 ± 0.72	-6.71 ± 0.22	0.9962
1-naphthylamine	-9.93 ± 0.22	-8.20 ± 0.71	-7.69 ± 0.22	0.9970
resorcinol	-2.67 ± 0.11	-1.56 ± 0.34	-2.26 ± 0.11	0.9908
<i>m</i> -cresol	-4.64 ± 0.12	-1.74 ± 0.38	-4.16 ± 0.12	0.9961
2,6-dimethylphenol	-6.09 ± 0.19	-3.08 ± 0.62	-5.25 ± 0.19	0.9939
2,6-dichlorophenol	-7.25 ± 0.21	-3.98 ± 0.67	-6.16 ± 0.21	0.9951
1-naphthol	-5.36 ± 0.12	-2.68 ± 0.37	-4.63 ± 0.12	0.9971
1-methylnaphthalene	-6.01 ± 0.14	-0.51 ± 0.43	-5.87 ± 0.14	0.9969
1-chloronaphthalene	-7.07 ± 0.22	-1.18 ± 0.71	-6.75 ± 0.22	0.9941